UC San Diego

UC San Diego Previously Published Works

Title

Genetic Identification of SEMA3F as an Antilymphangiogenic Metastasis Suppressor Gene in Head and Neck Squamous Carcinoma.

Permalink

https://escholarship.org/uc/item/76r320vd

Journal

Cancer Research, 75(14)

Authors

Doçi, Colleen

Mikelis, Constantinos

Lionakis, Michail

et al.

Publication Date

2015-07-15

DOI

10.1158/0008-5472.CAN-14-3121

Peer reviewed

eScholarship.org Powered by the California Digital Library
University of California

Author Manuscript

Author Manuscript

Author Manuscript

Author Manuscript

HHS Public Access

Author manuscript

Cancer Res. Author manuscript; available in PMC 2016 July 15.

Published in final edited form as:

Cancer Res. 2015 July 15; 75(14): 2937–2948. doi:10.1158/0008-5472.CAN-14-3121.

Genetic identification of SEMA3F as an anti-lymphangiogenic metastasis suppressor gene in head and neck squamous carcinoma

Colleen L. Doçi[1], **Constantinos M. Mikelis**[1], **Michail S. Lionakis**[2], **Alfredo A. Molinolo**[1], and **J. Silvio Gutkind**[1]

[1]Oral and Pharyngeal Cancer Branch, National Institute of Dental and Craniofacial Research, National Institutes of Health, 30 Convent Drive, Rm. 211, Bethesda, MD 20892, USA.

[2]Fungal Pathogenesis Unit, Laboratory of Clinical Infectious Diseases, National Institute of Allergy and Infectious Diseases, National Institutes of Health, Bethesda, MD 20892, USA.

Abstract

Head and neck squamous cell carcinomas (HNSCC) often metastasize to locoregional lymph nodes, and lymph node involvement represents one of the most important prognostic factors of poor clinical outcome. HNSCC are remarkably lymphangiogenic and represent a clear example of a cancer that utilizes the lymphatic vasculature for malignant dissemination; however, the molecular mechanisms underlying lymphangiogenesis in HNSCC is still poorly understood. Of interest, we found that an axon guidance molecule, *Semaphorin 3F* (*SEMA3F*), is among the top 1% underexpressed genes in HNSCC, and that genomic loss of *SEMA3F* correlates with increased metastasis and decreased survival. SEMA3F acts on its co-receptors, plexins and neuropilins, among which neuropilin-2 (NRP2) is highly expressed in lymphatic endothelial cells (LECs) but not in oral epithelium and most HNSCCs. We show that recombinant SEMA3F promotes LEC collapse and potently inhibits lymphangiogenesis *in vivo*. By reconstituting all possible plexin and neuropilin combinations, we found that SEMA3F acts through multiple receptors, but predominantly requires NRP2 to signal in LECs. Using orthotopic HNSCC metastasis mouse models, we provide direct evidence that *SEMA3F* re-expression diminishes lymphangiogenesis and lymph node metastasis. Furthermore, analysis of a large tissue collection revealed that SEMA3F is progressively lost during HNSCC progression, concomitant with increased tumor lymphangiogenesis. *SEMA3F* is localized to 3p21, an early and frequently deleted locus in HNSCC and many other prevalent human malignancies. Thus, *SEMA3F* may represent an antilymphangiogenic metastasis suppressor gene widely lost during cancer progression, hence serving as a prognostic biomarker and an attractive target for therapeutic intervention to halt metastasis.

Keywords

Metastasis; lymphangiogenesis; cancer; semaphorins; endothelial cell

Address correspondence to: J. Silvio Gutkind, Oral and Pharyngeal Cancer Branch, National Institute of Dental and Craniofacial Research, National Institutes of Health, 30 Convent Drive, Bldg 30, Rm 320, Bethesda, MD 20892, Tel.: +1-301-496-3695, sg39v@nih.gov.

Author Manuscript Author Manuscript Author Manuscript Author Manuscript

INTRODUCTION

One of the defining hallmarks of cancer is ability to form new vasculature to facilitate the growth and metastatic spread of cancer cells (1). Metastasis is the leading cause of morbidity in patients with a variety of solid tumors, where cancer cells often disseminate through blood and lymphatic vessels (1). Thus, the presence of intra- and peritumoral vasculature is a critical diagnostic and prognostic biomarker (2). Angiogenesis is required for tumors to grow beyond a critical limit and tumor-associated blood vessels have been suggested to participate in metastasis (3). Significantly less is known about the role of lymphangiogenesis in cancer, although lymphatic invasion is one of the most relevant diagnostic parameters for solid tumors (2,4,5). Specifically, melanoma and head and neck squamous cell carcinomas (HNSCC) demonstrate intratumoral lymphangiogenesis that is associated with invasion, metastasis, and decreased survival (6–8). However, the relative contribution of angiogenesis and lymphangiogenesis to cancer progression and metastasis is still not fully understood.

HNSCC is one of the ten most common cancers globally and less than half of patients diagnosed with nonlocalized disease will survive beyond five years (9,10). This is partially attributed to the propensity of HNSCC to metastasize to locoregional lymph nodes, which is the single most significant prognostic indicator and decreases the overall survival rate by more than 50% (11–13). Further, approximately 40% of the lymph nodes in the human body are located within the head and neck region (14), and HNSCC demonstrates significant intratumoral lymphangiogenesis compared to other solid cancers, suggesting that lymphangiogenesis may play a pivotal role in HNSCC metastasis and survival. Therefore, HNSCC may represent a clinically relevant condition to begin to dissect the specific role of lymphangiogenesis in metastasis.

The emergence of deep-sequencing approaches for human disease has led to the identification of a multitude of aberrant molecules in cancer that may contribute to its pathogenesis. While conducting analyses on altered molecules in the HNSCC genome, we observed that *SEMA3F* is among the top 1% underexpressed genes (15). SEMA3F is a member of the class 3 semaphorin family originally characterized in axonal guidance (16). In addition, semaphorins have been shown to play multiple roles in normal and pathologic angiogenesis by acting on their receptors, plexins and neuropilins (17–20). Interestingly, SEMA3F can bind to neuropilin 2 (NRP2), and early studies indicated that SEMA3F expression prevents the growth of metastatic melanoma cells that express high levels of NRP2 (21). However, the relevance of SEMA3F expression in cancers lacking NRP2 has not been investigated. Furthermore, NRP2 is a co-receptor highly expressed on LECs. Therefore, these observations prompted us to explore whether SEMA3F loss may contribute to HNSCC lymphangiogenesis, and hence impact on cancer progression and metastasis.

MATERIALS AND METHODS

The following represent a brief summary of the procedures. Please see the Supplemental Material for additional detailed methods.

Author Manuscript Author Manuscript Author Manuscript Author Manuscript

Cell Culture

293T-17, HaCat, COS-7, UMSCC2 and UMSCC17B cells were cultured in DMEM + 10% fetal bovine serum (FBS). LECs and HMVECs were cultured in EGM2-MV and HUVECs were cultured in EGM-2 (Lonza. All cells were cultured at 37°C in 5% CO_2. UMSCC2 and UMSCC17B stable cell lines were achieved by selection with 1 μg/ml blasticidin. Transfection of plasmids and siRNAs can be found in the supplemental methods. All cell lines underwent DNA authentication (Genetica DNA Laboratories, Inc.) before the described experiments to ensure consistency in cell identity.

TCGA analysis

Data regarding the copy number of *PIK3CA* and *SEMA3F* in head and neck cancer was downloaded from the cBio Portal for Cancer Genomics (http://www.cbioportal.org/public-portal/ accessed February 5, 2014).

Immunohistochemistry

Tissue arrays containing normal and oral cancer tissues were purchased from US BioMax Inc. Histopathology of tongue sections was performed as previously described (22). FFPE slides were stained and for tissue arrays were classified based on the intensity and the percentage of positive cells quantified as described (23). Correlations were determined using Pearson's Coefficient.

SEMA3F Purification

Serum-free CM from 293T-17 cells expressing NTAP-SEMA3F construct was collected, dialyzed, then isolated using HisTALON cobalt beads (Clontech). ΔFLAG control was generated by incubating purified SEMA3F with anti-FLAG conjugated beads (Sigma-Aldrich) and collecting the unbound supernatant.

Immunobloting

Cells were lysed in RIPA buffer and concentration was determined using Bio-Rad DC protein assay. Twenty micrograms total protein was separated by SDS-PAGE and transferred to PVDF membrane overnight at 4°C. Membranes were blocked for 1 hour at room temperature in 5% milk in TBST and then probed with primary antibodies overnight at 4°C. Membranes were washed four times in TBST, probed with HRP-conjugated secondary antibodies for 1h at RT in 5% milk, washed four times in TBST, and detected using chemiluminescent substrate (Millipore).

Immunofluorescence

For LECs and NOKs, cells were fixed with 4% paraformaldehyde and permeabilized with 0.1% Triton X-100. LECs were stained with phalloidin-GFP (Invitrogen) and counterstained with Hoescht 33342 (Invitrogen). NOKs were stained with SEMA3F (Sigma-Aldrich) or 58K Golgi Protein (Abcam), imaged with anti-rabbit AlexaFluor 488 (Invitrogen) or anti-goat AlexaFluor 546 (Invitrogen), and counterstained with Hoescht 33342 (Invitrogen). For matrigel and orthotopic tumor sections, FFPE slides were prepared and stained using the immunohistochemistry protocol described, and then counterstained Hoescht 33342

Author Manuscript Author Manuscript Author Manuscript Author Manuscript

(Invitrogen). The images were taken using an Axio Imager Z1 microscope equipped with an ApoTome system.

Cell adhesion and collapse assays

For adhesion assays, LEC were treated and plated on collagen-coated plates. Nonadherent cells were removed by washing and adherent cells fixed and stained. For collapse, LECs were transfected with LifeAct GFP and treated, or treated, fixed and stained with fluorescent phalloidin and nuclear counterstain. Cell area and perimeter were assessed using ImageJ. For heterologous assays, transfected COS-7 cells were treated as indicated. For all assays, quantification was performed using ImageJ from three independent experiments. Statistical significance was determined using one-way ANOVA. For movies, cells were imaged on an Olympus IX-81 inverted confocal microscope with images obtained every 30 seconds for a total of 3 hours, and analyzed using ZEN software (Carl Zeiss).

In vivo lymphangiogenesis assay and FACS

Basement membrane extract (Trevigen) plugs with growth factors and inhibitors, as indicated, were injected subcutaneously into the flank of nude mice. Single cell suspensions from plugs were prepared as described (24) and cell populations determined by FACS. Statistics were determined using ANOVA from three independent experiments. Cells were resuspended in PBS, stained with a LIVE/DEAD fluorescent dye (L-23105; Invitrogen), and incubated with CD16/32 (2.4G2; BD Biosciences) to block Fc receptors. For staining, cells were incubated with Alexa Fluor 488-conjugated LYVE-1, PE-Cy7-conjugated CD31, allophycocyanin (APC)-conjugated TER-119, APC-Cy7-conjugated CD45 and eFluor 450-conjugated CD102 (eBioscience or BD Biosciences) washed, and analyzed on a 5-laser LSRFortessa™ (BD Biosciences). Data were analyzed using FACS Diva (BD Biosciences) and FlowJo software (Treestar). Quantification of cell types was performed using PE-conjugated fluorescent counting beads (Spherotech).

Migration assay

Cells were treated as indicated for overnight Boyden migration. Membranes were fixed with methanol, counterstained with hematoxylin, and imaged on an Axiovert microscope. Calculations were based on 18 imaging fields each from three independent experiments. Statistical significance was determined using ANOVA.

Proliferation assay

Cancer cell lines were plated to 60% confluence and transferred to serum-free media with doxycycline for 20 hours. Cells were incubated an additional 4 hours with 1 μCi [methyl-^{3}H]-thymidine (Perkin-Elmer). Proliferation was determined by liquid scintillation counting. Statistical significance was determined using ANOVA.

Orthotopic tumor xenografts in SCID/NOD mice

All animal studies were carried out according to NIH-approved protocols (ASP# 10-569), in compliance with the NIH Guide for the Care and Use of Laboratory Animals. Female severe combined immunodeficient (SCID)/NOD mice (NCI) were housed in appropriate sterile

Author Manuscript Author Manuscript Author Manuscript Author Manuscript

filter-capped cages, and fed and watered *ad libitum*. Each animal was injected with 10^5 cells in 50 μl of serum-free media in the tongue. Animals in the control group were fed regular chow, while animals in the prevention group were fed 6g doxycycline/kg chow one week prior to injection and throughout the study. All animals underwent evaluation of the tongue for disease onset every three days, and the observed lesions were assessed for length and width, and tumor volume was determined as described previously (22). Animals were euthanized at the indicated time points and the cervical lymph nodes assessed for evidence of metastases by H&E staining.

RESULTS

SEMA3F expression is lost during HNSCC progression

While analyzing gene expression alterations in HNSCC in available datasets, we observed that *SEMA3F* is among the 1% most downregulated genes [−2.09 fold decrease, p=3.6E-20 (15)] and is localized to 3p21, one of the most commonly deleted loci in HNSCC (25). To investigate whether reduced *SEMA3F* expression is caused by genomic alterations, we interrogated the TCGA Head and Neck Cancer databases, using *PIK3CA*, one the most frequently amplified genes in HNSCC that is localized to the long arm of the same chromosome (26) as a control (Figure 1A). Nearly 75% of HNSCC patients showed heterozygous loss of *SEMA3F*, suggesting that this semaphorin may represent a potential tumor suppressor (Fig. 1A). We assessed the Kaplan-Meier univariate survival of patients with heterozygous loss of *SEMA3F* (Fig. 1B) and the Cox Proportional Hazard multivariate survival, taking into consideration lymph node metastasis (Fig 1C). In both analyses, SEMA3F was a strong negative indicator of survival and a statistically significant independent biomarker (HR= 2.1, p=0.01 and exp(β)=1.95, p = 0.03, respectively). The median survival of patients with heterozygous loss was nearly half of patients expressing normal levels of *SEMA3F* (Fig. 1D). Additionally, patients with *SEMA3F* heterozygous loss showed significantly increased percentage of metastatic lymph nodes and lymphovascular invasion (Fig.1E and 1F).

SEMA3F loss was reflected at the protein level, as immunohistochemical evaluation of SEMA3F using a SEMA3F-specific antibody (Supplementary Fig, 1) revealed progressive loss of expression with advancing cancer severity. While normal oral epithelium demonstrated high level of SEMA3F expression, this was almost completely abolished in advanced cancers (Fig. 1G). Quantification of a large collection of HNSCC tissues revealed that nearly 70% of the proliferating basal cells in normal oral epithelium expressed high levels of SEMA3F, while over half of HNSCC samples express little to no SEMA3F (Fig. 1H). Interestingly, this correlated with enhanced tumor vascularity, with markers for blood and lymphatic endothelium significantly increased in the absence of SEMA3F (Fig. 1I and Supplementary Fig. 2). These data support that decreased expression of SEMA3F correlates with poor clinical outcome, increased tumor vascularity, invasion, and metastasis, thus suggesting that SEMA3F may function as a tumor and metastasis suppressor in HNSCC.

Author Manuscript Author Manuscript Author Manuscript Author Manuscript

SEMA3F is a chemorepulsant for lymphatic endothelial cells

As the SEMA3F co-receptor NRP2 is highly expressed on LECs (27), we asked whether SEMA3F has a functional impact on these endothelial cells. We engineered a SEMA3F construct that would preserve its extracellular secretion and posttranslational processing while allowing for coexpression of N-terminal tandem affinity purification (NTAP) tags (Fig. 2A). SEMA3F was expressed, fully processed, and the secreted form of the protein was capable of purification using histidine affinity resin (Fig. 2A). Class 3 semaphorins function through a mechanism that involves negative regulation of integrin adhesion to the extracellular matrix, thereby modulating the attachment of endothelial cells to extracellular matrices through cytoskeletal remodeling (28). Secreted SEMA3F was functionally active in HUVEC adhesion assays, and this effect is specific as FLAG-depleted SEMA3F conditioned media (CM) but not IgG-depeleted CM was no longer able to inhibit attachment (Fig. 2B). Furthermore, SEMA3F caused a dose-dependent decrease of LEC attachment which was abolished by FLAG-mediated depletion (Fig. 2C). SEMA3F also induced a nearly 80% collapse of the LEC actin cytoskeleton, while decreasing cell perimeter by less than 3% (Fig. 2D). Using either purified SEMA3F or FLAG-depleted control, we documented the cellular collapse using live-cell imaging in LECs expressing fluorescent actin (Supplementary Movies 1 and 2). SEMA3F induced significant retraction of the LEC cytoskeleton, while little change in actin was observed in the FLAG-depleted control (Fig. 2E). Together, this indicates that SEMA3F can be purified in a biologically active form that is capable of negatively regulating the function of LECs.

SEMA3F inhibits LEC function in vivo

We next asked whether SEMA3F can function as antilymphangiogenic factor *in vivo*. Matrigel combined with different growth factors were implanted in flanks of nude mice and invaded cells were identified and quantified by FACS. As proangiogenic growth factors such as vascular endothelial growth factor (VEGF) -A and –C use neuropilins as co-receptors (16), sphingosine-1-phosphate (S1P) and basic fibroblast growth factor (bFGF) were substituted to circumvent any potential competition with SEMA3F. A stepwise gating strategy was employed to identify specific types of vascular-associated cells and endothelial cells while excluding immune-reactive cells like macrophages (Supplementary Fig. 3). Using matrigel alone as a negative control and S1P and bFGF as a positive control, we tested the ability of purified SEMA3F to block chemoattractant-mediated endothelial cell recruitment in a dose-dependent, quantitative *in vivo* setting (Fig. 3).

Gross evaluation and H&E staining matrigel plugs demonstrated strong infiltration of vasculature in the positive control that was attenuated by SEMA3F addition (Fig. 3A, upper and middle panels). Immunofluorescence against vascular (CD31) and lymphatic (LYVE-1) vessels demonstrate a SEMA3F dose-dependent decrease in S1P- and bFGF-induced vessel recruitment (Fig. 3A, lower panels). SEMA3F caused approximately 70% decrease in the abundance of red blood cells, long-regarded as the standard for angiogenesis implantation assays (Fig. 3B) (29). Similarly, we saw 60–70% decreased abundance of total $CD31^+$ $CD102^+$ endothelial cells (Fig. 3C) and vascular endothelial cells expressing little to no LYVE-1 ($LYVE\text{-}1^{low}$), consistent with an antiangiogenic function previously reported for SEMA3F (21,30,31) (Fig. 3D). Remarkably, SEMA3F prevented the recruitment of LECs

Author Manuscript Author Manuscript Author Manuscript Author Manuscript

(defined as LYVE-1^{hi}), with a 70–85% reduction in the abundance of LECs with respect to control plugs (Fig. 3E). Thus, SEMA3F has potent antiangiogenic activity and an even more robust antilymphangiogenic function.

NRP and Plexin A coreceptor complexes are sufficient for SEMA3F signaling

NRP2 and Plexin A family members are capable of binding to SEMA3F (32,33), but the relative contribution of each member of this family to SEMA3F-mediated signaling is unknown. Primary human umbilical vein endothelial cells (HUVEC), human microvascular endothelial cells (HMVEC), and LEC express NRP1, NRP2, and Plexin A family members to varying degrees, while COS-7 cells do not express any of these receptors endogenously, thus serving as a heterologous system to investigate SEMA3F signaling (Fig. 4A). Each of the NRP and Plexin A family members were expressed in COS-7 cells to test their relative contribution to SEMA3F signaling alone and in coreceptor complexes (Fig. 4B). As a control, we also tested the effect of SEMA3A, as this semaphorin signals primarily through NRP1-Plexin A1 and NRP1-Plexin A3 (34).

Neither NRPs nor Plexins alone were sufficient for SEMA3F or SEMA3A signaling (Fig.4C and 4D). SEMA3A was most effective in cells expressing NRP1 and Plexin A1, as predicted. SEMA3F potently induced the collapse of COS-7 cells that expressed NRP2 and Plexin A3, although cells expressing NRP2 and Plexin A1 also collapsed when compared to controls. Interestingly, a modest collapse was observed in SEMA3F-treated cells that expressed NRP1 and Plexin A3, and to a lesser degree in those that expressed NRP1 and Plexin A1. Some broader effect of SEMA3A was also observed, as NRP2-Plexin A1 complexes and NRP1-Plexin A4 complexes showed collapse. Plexin D1, a receptor for SEMA3E, did not appear to play a role in SEMA3F function (Supplementary Fig. 4). Based on these results, we summarized the relative contribution of different receptor combinations to SEMA3F-induced cytoskeletal collapse (Fig. 4E). Finally, we performed live cell imaging of the collapse in COS-7 cells transfected with NRP2 control or NRP2 and Plexin A3 treated with SEMA3F (Supplementary Movies 3–4). Control cells demonstrated no changes in the actin cytoskeleton, while expression of NRP2 and Plexin A3 was sufficient to induce a rapid collapse phenotype with significant alterations in the actin cytoskeleton (Fig. 4F).

NRP2 is predominantly required for SEMA3F signaling

To determine whether both endogenous NRP1 and NRP2 are necessary for SEMA3F signaling, we abolished expression of these receptors using siRNAs in LECs. Little to no NRP expression remained in siRNA-targeted cells, with no apparent cross-specificity between the knockdown sequences (Fig. 5A). Loss of NRP1 expression only modestly attenuated the collapse of the cells upon SEMA3F treatment; however, significantly less collapse was observed in SEMA3F-treated LEC that do not express NRP2 (Fig. 5B). In a dose-response collapse (Fig. 5C) and attachment (Fig. 5D) assay, loss of NRP1 slightly inhibited the effectiveness of low doses of SEMA3F. In both assays, however, NRP2 knockdown had a pronounced effect, suggesting that NRP2 is the dominant SEMA3F receptor in LECs. This was further documented by log-dose response analysis (Fig. 5E). While loss of NRP1 increased the IC_{50} of SEMA3F slightly compared to control, NRP2-deficient cells required nearly ten times more SEMA3F to achieve the same effect. Taken

Author Manuscript Author Manuscript Author Manuscript Author Manuscript

together, these findings suggest that while NRP1 may play a role in transmitting SEMA3F signal in the absence of NRP2, NRP2 is predominately required for SEMA3F biological responses in LECs.

A subset of HNSCC cells express NRP2, and respond to the anti-tumor activity of SEMA3F

Normal oral keratinocytes and most HNSCC cancer cells do not express NRP1 or NRP2. However, a subset of HNSCC cell lines acquired expression of NRP2 (Fig. 6A). Aligned with this observation, increased NRP2 mRNA expression correlates with loss of SEMA3F ($p = 0.003$), poor prognosis, and decreased survival (Supplementary Figure 5). To test the effect of SEMA3F in HNSCC cells with or without NRP2, we chose two representative highly tumorigenic and metastatic HNSCC cell lines (22), UMSCC17B, which do not express NRPs, and UMSCC2, with high level expression of NRP2. As an experimental approach, we used a doxycycline-inducible system and confirmed that doxycycline addition induced SEMA3F expression without changing the expression of NRP1 or NRP2 in these cells (Fig. 6B). In both cell types, expression of the rtTA3 tetracycline-dependent transactivating complex alone had no effect on proliferation (Fig.6C and 6D). SEMA3F expression inhibited proliferation of UMSCC2 cells significantly; however, this effect was abrogated upon NRP2 knockdown (Fig. 6C). Conversely, in UMSCC17B cells induction of SEMA3F did not alter proliferation (Fig. 6D). As a gain of function strategy, transient expression of NRP2 in UMSCC17B rendered them sensitive to the growth inhibitory activity of SEMA3F (Fig. 6D).

Induction of SEMA3F in UMSCC2 cells also blocked endogenous and directed migration (Fig. 6E). Interestingly, siRNA-mediated loss of NRP2 decreased the endogenous migration of these cells compared to control siRNA, although there was no difference between vehicle and doxycyline-treated groups (Fig. 6E). Ectopic expression of NRP2 in UMSCC17B cells was sufficient to enhance cell migration over vector control, and induction of SEMA3F did not alter endogenous UMSCC17B migration unless NRP2 was introduced to these cells (Fig. 6F). Taken together, this supports that HNSCC cells expressing NRP2 may exhibit increased migratory capacity, but that loss of SEMA3F may need to precede gain of NRP2 expression.

SEMA3F functions as a potent HNSCC metastasis suppressor

SEMA3F inhibited the biologic activity of LECs and intratumoral lymphangiogenesis is highly prevalent in HNSCC, suggesting that SEMA3F may suppress metastasis *in vivo* through paracrine mechanisms. To test this hypothesis in the context of NRP2 expression or absence, we injected UMSCC2-rtTA3-SEMA3F and UMSCC17B-rtTA3-SEMA3F cells into the tongues of mice and assessed tumor growth, metastasis, and intratumoral vascularity. Consistent with our observations *in vitro*, doxycycline induction of rtTA3 alone had no effect on tumor growth (Supplementary Fig 6). SEMA3F induction inhibited tumor growth in the UMSCC2-injected animals (Fig. 7A) and this correlated with a statistically significant decrease in cervical lymph node metastasis (Fig. 7C). Interestingly, SEMA3F induction in UMSCC17B tumors, which do not express NRP2, had no effect on tumor size (Fig. 7B). However, a similar decrease in lymph node metastasis was observed (Fig. 7D). This suggested that the paracrine signaling of SEMA3F to the tumor stroma may be

Author Manuscript Author Manuscript Author Manuscript Author Manuscript

sufficient for suppression of metastasis, while exerting an additional autoinhibitory effect on tumor growth in HNSCC cells that acquired expression of NRP2.

Tongue sections were evaluated by immunohistochemistry for CD31 and LYVE1 and the intratumoral microvessel density (MVD) was quantified. In both the UMSCC2 and UMSCC17B tumors, induction of SEMA3F significantly decreased intratumoral lymphangiogenesis and modestly decreased CD31+ vasculature, albeit not to a statistically significant degree (Fig.7E and 7F). As a control, MVD outside the tumor was quantified and was not affected for either CD31 or LYVE1 (Fig.7E and 7F). Immunofluorescence staining revealed a high rate of cancer cells infiltrating into lymphatic vessels in control animals that were not observed in SEMA3F-induced cohorts (Fig.7G and 7H, white arrows). These results demonstrate that SEMA3F exerts a potent antilymphangiogenic and metastasis suppressor function in HNSCC, and that SEMA3F may also inhibit growth of a subset of HNSCC expressing NRP2.

DISCUSSION

The tumor microenvironment is regulated through a complex autocrine and paracrine signaling network that is often hijacked and exploited by cancer cells to facilitate their survival, growth and dissemination. In HNSCC the interplay of these factors is shifted to promote intratumoral lymphangiogenesis and metastasis, which contribute to poor prognosis and outcome (6,8). Our findings suggest that SEMA3F is a key antilymphangiogenic molecule that may function at the core of these cell regulatory networks during HNSCC progression. Indeed, loss of SEMA3F is a frequent event in HNSCC, which correlates with increased tumor vascularity and metastasis. We show that SEMA3F can directly affect LEC function *in vitro* and *in vivo* through specific receptor complexes. In COS-7 reconstitution assays, NRP2 and Plexin A3 were sufficient to mediate SEMA3F biological responses, while NRP2-Plexin A1, NRP1-Plexin A3, and NPR1-Plexin A1 complexes can also transduce SEMA3F signals, albeit with decreasing efficiency. NRP2 is the major co-receptor for SEMA3F in LECs, although NRP1 can transmit SEMA3F signals to a lesser extent. Overall, our *in vitro* and *in vivo* studies indicate that SEMA3F is potent anti-lymphangiogenic molecule. Thus, SEMA3F loss may represent an early event in HNSCC, enabling intratumoral lymphangiogenesis that may contribute to the high prevalence of HNSCC cases presenting with locoregional lymph node invasion, heralding a poor clinical outcome.

NRP2 is a multiligand co-receptor that can both promote and inhibit the development of venous and lymphatic vasculature, in the stroma and on some tumor cells themselves (35–37). In endothelial cells, NRP2 associates with Plexin A family members and VEGFR2 and VEGFR3, and these complexes have been implicated in their pro-angiogenic and –lymphangiogenic signaling (38,39). Certain malignant epithelial cells express NRP2 without concomitant expression of VEGF receptors (40). The observation that NRP2 but not VEGF receptors are expressed in a subset of HNSCC cells raises the possibility that in these cells NRP2 may act as a co-receptor for plexins or other partners, acting as a gain-of-function alteration during cancer development and progression. Indeed, exogenous NRP2 expression in HNSCC cells enhanced their endogenous migration while loss of upregulated NRP2 in

Author Manuscript Author Manuscript Author Manuscript Author Manuscript

HNSCC cells decreased their endogenous migration. This allows us to hypothesize that cancer cells may be selected for their NRP2 expression due to an increased growth or migratory potential, but that *SEMA3F* loss may need to precede NRP2 gain in HNSCC (Fig 7I).

Lymphatic metastasis is mainly attributed to increased expression and signaling of pro-angiogenic factors (2,5,41–43). However, expression and secretion of these growth factors alone may not be sufficient for tumor-associated lymphangiogenesis and cancer dissemination. For example, in some cancers VEGF-C or VEGF-D expression levels do not correlate with lymph node metastasis (44,45), suggesting that other factors may counteract the high level expression of pro-lymphangiogenic cytokines and attenuate their signaling capacity and prognostic value *in vivo*. Based on our present results, one possible explanation is that SEMA3F could repel LECs and thus dominate the activity of VEGF-A and VEGF-C, rendering their expression alone insufficient for lymphangiogenesis and metastasis. This hypothesis is supported by our findings that induction of SEMA3F alone in orthotopic HNSCC cells significantly inhibits intratumoral lymphangiogenesis and metastasis, even in HNSCC cells that do not express NRP2. Thus, loss of SEMA3F expression in HNSCC may simultaneously enhance VEGF-mediated signaling on endothelial cells and alleviate repressive semaphorin functions resulting in increased lymphangiogenesis.

Our observation may have a broad impact in multiple highly prevalent human malignancies. In an integrative multiplatform analysis, 3p deletion was identified as a key genomic signature shared by a squamous-like subtype of solid cancers (46). Further, chromosomal loss at 3p21, which is expected to result in the genomic deletion of *SEMA3F*, has been observed for lung, breast, and kidney cancers in addition to HNSCC (47–50). Immunohistochemistry on HNSCC tumors reveals a complete absence of SEMA3F expression in most advanced cases, suggesting that epigenetic regulation or transcriptional dowregulation may contribute to reduced SEMA3F expression of the remaining *SEMA3F* allele in cancers with *SEMA3F* heterozygous loss. We can conclude that SEMA3F is a potent chemorepellent molecule for lymphatic and vascular endothelial cells, which acts through NRP2-Plexin A and to a lesser extent NRP1-Plexin A signaling complexes. Loss of *SEMA3F* is an early event in HNSCC and likely many other highly prevalent human malignancies. This information can in turn be exploited for therapeutic purposes, as most HNSCC lesions may retain one intact *SEMA3F* allele. This suggests that reactivation of SEMA3F expression or ectopic SEMA3F delivery may offer the opportunity to halt intratumoral lymphangiogenesis and suppress metastasis regardless of the NRP2 expression status of the HNSCC lesion. We can conclude that SEMA3F-NRP2 represents a novel regulatory axis during HNSCC development, progression, and metastasis, thus providing new prognostic markers and therapeutic options in this highly aggressive disease.

Supplementary Material

Refer to Web version on PubMed Central for supplementary material.

Author Manuscript Author Manuscript Author Manuscript Author Manuscript

ACKNOWLEDGEMENTS

We thank Dr. Roberto Weigert for providing the LifeAct plasmid. We also thank Dr. Gera Neufeld for providing Plexin A1, A3, and A4 receptor plasmids and purified Sema3E.

Financial Support: This research was supported by the Intramural Research Program of the National Institute of Dental and Craniofacial Research, and in part by the National Institute of Allergy & Infectious Diseases, NIH (Z01DE00558-23 and Z01DE00551-23).

REFERENCES

1. Hanahan D, Weinberg RA. Hallmarks of cancer: the next generation. Cell. 2011; 144(5):646–674. [PubMed: 21376230]
2. Alitalo K, Tammela T, Petrova TV. Lymphangiogenesis in development and human disease. Nature. 2005; 438(7070):946–953. [PubMed: 16355212]
3. Folkman J. Angiogenesis: an organizing principle for drug discovery? Nat Rev Drug Discov. 2007; 6(4):273–286. [PubMed: 17396134]
4. Sundar SS, Ganesan TS. Role of lymphangiogenesis in cancer. J Clin Oncol. 2007; 25(27):4298–4307. [PubMed: 17878481]
5. Karaman S, Detmar M. Mechanisms of lymphatic metastasis. The Journal of Clinical Investigation. 2014; 124(3):922–928. [PubMed: 24590277]
6. Beasley NJ, Prevo R, Banerji S, Leek RD, Moore J, van Trappen P, et al. Intratumoral lymphangiogenesis and lymph node metastasis in head and neck cancer. Cancer Research. 2002; 62(5):1315–1320. [PubMed: 11888898]
7. Dadras SS, Lange-Asschenfeldt B, Velasco P, Nguyen L, Vora A, Muzikansky A, et al. Tumor lymphangiogenesis predicts melanoma metastasis to sentinel lymph nodes. Modern Pathology. 2005; 18(9):1232–1242. [PubMed: 15803182]
8. Kyzas PA, Geleff S, Batistatou A, Agnantis NJ, Stefanou D. Evidence for lymphangiogenesis and its prognostic implications in head and neck squamous cell carcinoma. The Journal of Pathology. 2005; 206(2):170–177. [PubMed: 15846845]
9. DeSantis CE, Lin CC, Mariotto AB, Siegel RL, Stein KD, Kramer JL, et al. Cancer treatment and survivorship statistics, 2014. CA Cancer J Clin. 2014
10. Siegel R, Ma J, Zou Z, Jemal A. Cancer statistics, 2014. CA Cancer J Clin. 2014; 64(1):9–29. [PubMed: 24399786]
11. Forastiere A, Koch W, Trotti A, Sidransky D. Head and neck cancer. N Engl J Med. 2001; 345(26):1890–1900. [PubMed: 11756581]
12. Leemans CR, Tiwari R, Nauta JJ, van der Waal I, Snow GB. Recurrence at the primary site in head and neck cancer and the significance of neck lymph node metastases as a prognostic factor. Cancer. 1994; 73(1):187–190. [PubMed: 8275423]
13. Shah JP, Candela FC, Poddar AK. The patterns of cervical lymph node metastases from squamous carcinoma of the oral cavity. Cancer. 1990; 66(1):109–113. [PubMed: 2354399]
14. Harisinghani, M. Head and Neck Lymph Node Anatomy. In: Harisinghani, MG., editor. Atlas of Lymph Node Anatomy. New York: Springer; 2013. p. 1-29.
15. Rhodes DR, Yu J, Shanker K, Deshpande N, Varambally R, Ghosh D, et al. ONCOMINE: a cancer microarray database and integrated data-mining platform. Neoplasia. 2004; 6(1):1–6. [PubMed: 15068665]
16. Carmeliet P, Tessier-Lavigne M. Common mechanisms of nerve and blood vessel wiring. Nature. 2005; 436(7048):193–200. [PubMed: 16015319]
17. Sakurai A, Doci CL, Gutkind JS. Semaphorin signaling in angiogenesis, lymphangiogenesis and cancer. Cell Res. 2012; 22(1):23–32. [PubMed: 22157652]
18. Gaur P, Bielenberg DR, Samuel S, Bose D, Zhou Y, Gray MJ, et al. Role of class 3 semaphorins and their receptors in tumor growth and angiogenesis. Clinical Cancer Research. 2009; 15(22): 6763–6770. [PubMed: 19887479]

Author Manuscript Author Manuscript Author Manuscript Author Manuscript

19. Neufeld G, Kessler O. The semaphorins: versatile regulators of tumour progression and tumour angiogenesis. Nat Rev Cancer. 2008; 8(8):632–645. [PubMed: 18580951]
20. Tessier-Lavigne M, Goodman CS. The molecular biology of axon guidance. Science. 1996; 274(5290):1123–1133. [PubMed: 8895455]
21. Bielenberg DR, Hida Y, Shimizu A, Kaipainen A, Kreuter M, Kim CC, et al. Semaphorin 3F, a chemorepulsant for endothelial cells, induces a poorly vascularized, encapsulated, nonmetastatic tumor phenotype. J Clin Invest. 2004; 114(9):1260–1271. [PubMed: 15520858]
22. Patel V, Marsh CA, Dorsam RT, Mikelis CM, Masedunskas A, Amornphimoltham P, et al. Decreased lymphangiogenesis and lymph node metastasis by mTOR inhibition in head and neck cancer. Cancer research. 2011; 71(22):7103–7112. [PubMed: 21975930]
23. Amornphimoltham P, Leelahavanichkul K, Molinolo A, Patel V, Gutkind JS. Inhibition of Mammalian target of rapamycin by rapamycin causes the regression of carcinogen-induced skin tumor lesions. Clinical Cancer Research. 2008; 14(24):8094–8101. [PubMed: 19073969]
24. Nagahashi M, Ramachandran S, Kim EY, Allegood JC, Rashid OM, Yamada A, et al. Sphingosine-1-phosphate produced by sphingosine kinase 1 promotes breast cancer progression by stimulating angiogenesis and lymphangiogenesis. Cancer Research. 2012; 72(3):726–735. [PubMed: 22298596]
25. Marescalco MS, Capizzi C, Condorelli DF, Barresi V. Genome-wide analysis of recurrent copy-number alterations and copy-neutral loss of heterozygosity in head and neck squamous cell carcinoma. Journal of Oral Pathology & Medicine. 2014; 43(1):20–27. [PubMed: 23750501]
26. Woenckhaus J, Steger K, Werner E, Fenic I, Gamerdinger U, Dreyer T, et al. Genomic gain of PIK3CA and increased expression of p110alpha are associated with progression of dysplasia into invasive squamous cell carcinoma. The Journal of Pathology. 2002; 198(3):335–342. [PubMed: 12375266]
27. Yuan L, Moyon D, Pardanaud L, Breant C, Karkkainen MJ, Alitalo K, et al. Abnormal lymphatic vessel development in neuropilin 2 mutant mice. Development. 2002; 129(20):4797–4806. [PubMed: 12361971]
28. Serini G, Valdembri D, Zanivan S, Morterra G, Burkhardt C, Caccavari F, et al. Class 3 semaphorins control vascular morphogenesis by inhibiting integrin function. Nature. 2003; 424(6947):391–397. [PubMed: 12879061]
29. Passaniti A, Taylor RM, Pili R, Guo Y, Long PV, Haney JA, et al. A simple, quantitative method for assessing angiogenesis and antiangiogenic agents using reconstituted basement membrane, heparin, and fibroblast growth factor. Laboratory investigation; a journal of technical methods and pathology. 1992; 67(4):519–528.
30. Guttmann-Raviv N, Shraga-Heled N, Varshavsky A, Guimaraes-Sternberg C, Kessler O, Neufeld G. Semaphorin-3A and semaphorin-3F work together to repel endothelial cells and to inhibit their survival by induction of apoptosis. J Biol Chem. 2007; 282(36):26294–26305. [PubMed: 17569671]
31. Guo HF, Li X, Parker MW, Waltenberger J, Becker PM, Vander Kooi CW. Mechanistic basis for the potent anti-angiogenic activity of semaphorin 3F. Biochemistry. 2013; 52(43):7551–7558. [PubMed: 24079887]
32. Xiang X, Zhang X, Huang QL. Plexin A3 is involved in semaphorin 3F-mediated oligodendrocyte precursor cell migration. Neurosci Lett. 2012; 530(2):127–132. [PubMed: 23063687]
33. Giger RJ, Urquhart ER, Gillespie SK, Levengood DV, Ginty DD, Kolodkin AL. Neuropilin-2 is a receptor for semaphorin IV: insight into the structural basis of receptor function and specificity. Neuron. 1998; 21(5):1079–1092. [PubMed: 9856463]
34. Takahashi T, Fournier A, Nakamura F, Wang LH, Murakami Y, Kalb RG, et al. Plexin-neuropilin-1 complexes form functional semaphorin-3A receptors. Cell. 1999; 99(1):59–69. [PubMed: 10520994]
35. Klagsbrun M, Eichmann A. A role for axon guidance receptors and ligands in blood vessel development and tumor angiogenesis. Cytokine Growth Factor Rev. 2005; 16(4–5):535–548. [PubMed: 15979925]

Author Manuscript Author Manuscript Author Manuscript Author Manuscript

36. Guttmann-Raviv N, Kessler O, Shraga-Heled N, Lange T, Herzog Y, Neufeld G. The neuropilins and their role in tumorigenesis and tumor progression. Cancer letters. 2006; 231(1):1–11. [PubMed: 16356825]
37. Rizzolio S, Tamagnone L. Multifaceted role of neuropilins in cancer. Curr Med Chem. 2011; 18(23):3563–3575. [PubMed: 21756227]
38. Xu Y, Yuan L, Mak J, Pardanaud L, Caunt M, Kasman I, et al. Neuropilin-2 mediates VEGF-C-induced lymphatic sprouting together with VEGFR3. J Cell Biol. 2010; 188(1):115–130. [PubMed: 20065093]
39. Appleton BA, Wu P, Maloney J, Yin J, Liang WC, Stawicki S, et al. Structural studies of neuropilin/antibody complexes provide insights into semaphorin and VEGF binding. The EMBO Journal. 2007
40. Wild JR, Staton CA, Chapple K, Corfe BM. Neuropilins: expression and roles in the epithelium. Int J Exp Pathol. 2012; 93(2):81–103. [PubMed: 22414290]
41. Mandriota SJ, Jussila L, Jeltsch M, Compagni A, Baetens D, Prevo R, et al. Vascular endothelial growth factor-C-mediated lymphangiogenesis promotes tumour metastasis. The EMBO Journal. 2001; 20(4):672–682. [PubMed: 11179212]
42. Stacker SA, Caesar C, Baldwin ME, Thornton GE, Williams RA, Prevo R, et al. VEGF-D promotes the metastatic spread of tumor cells via the lymphatics. Nature Medicine. 2001; 7(2): 186–191.
43. Cao R, Ji H, Feng N, Zhang Y, Yang X, Andersson P, et al. Collaborative interplay between FGF-2 and VEGF-C promotes lymphangiogenesis and metastasis. Proceedings of the National Academy of Sciences of the United States of America. 2012; 109(39):15894–15899. [PubMed: 22967508]
44. Lahat G, Lazar A, Wang X, Wang WL, Zhu QS, Hunt KK, et al. Increased vascular endothelial growth factor-C expression is insufficient to induce lymphatic metastasis in human soft-tissue sarcomas. Clinical Cancer Research. 2009; 15(8):2637–2646. [PubMed: 19351758]
45. Ishikawa M, Kitayama J, Kazama S, Nagawa H. Expression of vascular endothelial growth factor C and D (VEGF-C and -D) is an important risk factor for lymphatic metastasis in undifferentiated early gastric carcinoma. Jpn J Clin Oncol. 2003; 33(1):21–27. [PubMed: 12604720]
46. Hoadley KA, Yau C, Wolf DM, Cherniack AD, Tamborero D, Ng S, et al. Multiplatform Analysis of 12 Cancer Types Reveals Molecular Classification within and across Tissues of Origin. Cell. 2014; 158(4):929–944. [PubMed: 25109877]
47. Kok K, Naylor SL, Buys CH. Deletions of the short arm of chromosome 3 in solid tumors and the search for suppressor genes. Advances in Cancer Research. 1997; 71:27–92. [PubMed: 9111863]
48. Sekido Y, Ahmadian M, Wistuba II, Latif F, Bader S, Wei MH, et al. Cloning of a breast cancer homozygous deletion junction narrows the region of search for a 3p21.3 tumor suppressor gene. Oncogene. 1998; 16(24):3151–3157. [PubMed: 9671394]
49. Roche J, Boldog F, Robinson M, Robinson L, Varella-Garcia M, Swanton M, et al. Distinct 3p21.3 deletions in lung cancer and identification of a new human semaphorin. Oncogene. 1996; 12(6): 1289–1297. [PubMed: 8649831]
50. Hesson LB, Cooper WN, Latif F. Evaluation of the 3p21.3 tumour-suppressor gene cluster. Oncogene. 2007; 26(52):7283–7301. [PubMed: 17533367]

Author Manuscript Author Manuscript Author Manuscript Author Manuscript

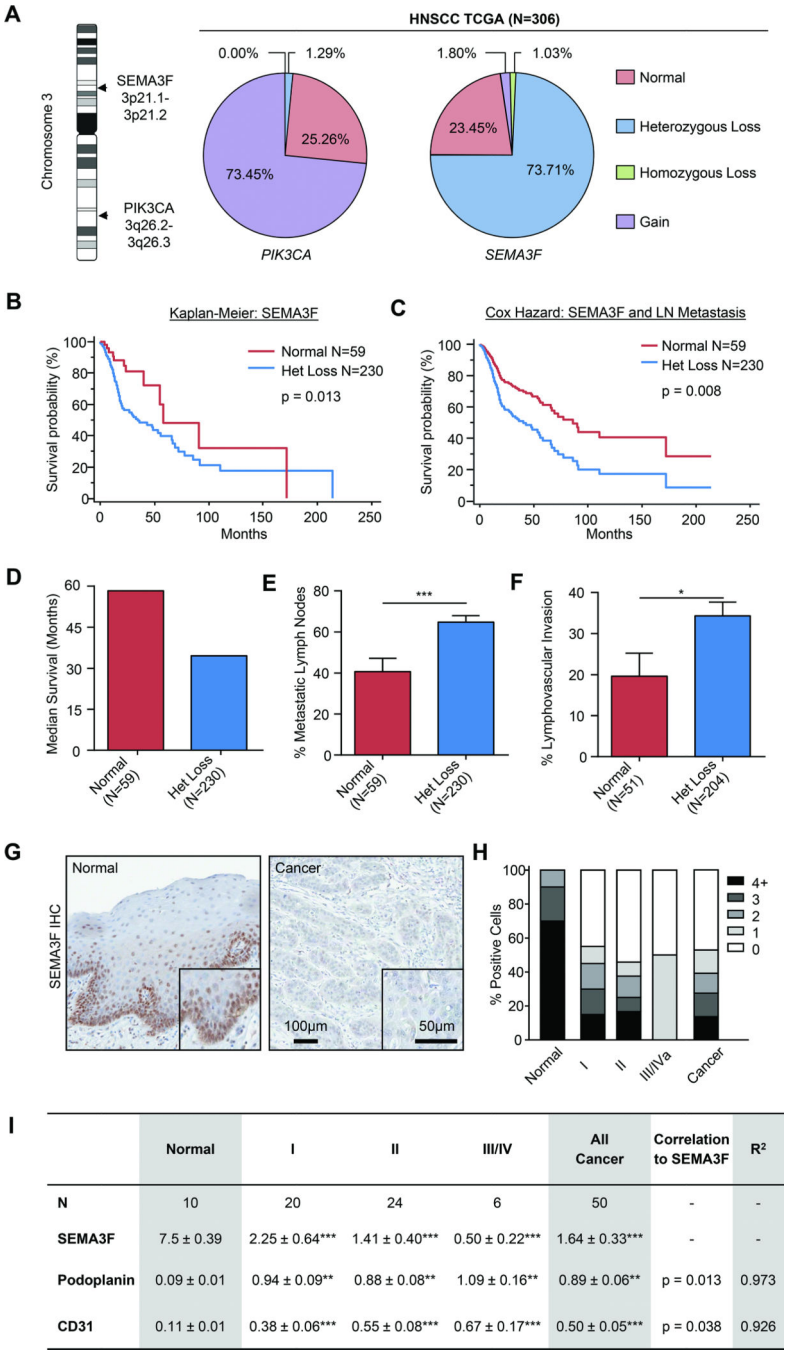

I

	Normal	I	II	III/IV	All Cancer	Correlation to SEMA3F	R^2
N	10	20	24	6	50	-	-
SEMA3F	7.5 ± 0.39	2.25 ± 0.64***	1.41 ± 0.40***	0.50 ± 0.22***	1.64 ± 0.33***	-	-
Podoplanin	0.09 ± 0.01	0.94 ± 0.09**	0.88 ± 0.08**	1.09 ± 0.16**	0.89 ± 0.06**	p = 0.013	0.973
CD31	0.11 ± 0.01	0.38 ± 0.06***	0.55 ± 0.08***	0.67 ± 0.17***	0.50 ± 0.05***	p = 0.038	0.926

Fig. 1. SEMA3F expression is lost during head and neck cancer progression

A) *SEMA3F* (3p21.1–3p21.2) and *PIK3CA* (3q26.2-2q26.3) are located on Chromosome 3 and their genomic copy number in head and neck cancer patients according to TCGA was calculated. Clinical outcome for patients with normal (CN=2) or *SEMA3F* heterozygous loss (CN=1) were interrogated and Kaplan-Meier (B) and Cox Proportional Hazard survival curves (C), median survival (D) evidence of metastatic disease (E), and lymphovascular invasion (F) were determined. G) Immunohistochemistry of SEMA3F in primary tumor sections of normal oral epithelium and cancer. H) Quantification of SEMA3F staining in a

Author Manuscript Author Manuscript Author Manuscript Author Manuscript

tissue array including normal oral epithelium, Stage I, II, III and IV cancers cases. Tissues were evaluated for intensity and percentage of positive cells, with 0 being absent staining and 4+ being intense staining in all cells. I) The same array was also stained for podoplanin (lymphatic vessels) and CD31 (blood vessels) and correlation to SEMA3F expression was calculated using Pearson's Coefficient. Statistical significance compared to normal was determined by Student's t-test, **$p<0.01$, ***$p<0.001$.

Author Manuscript Author Manuscript Author Manuscript Author Manuscript

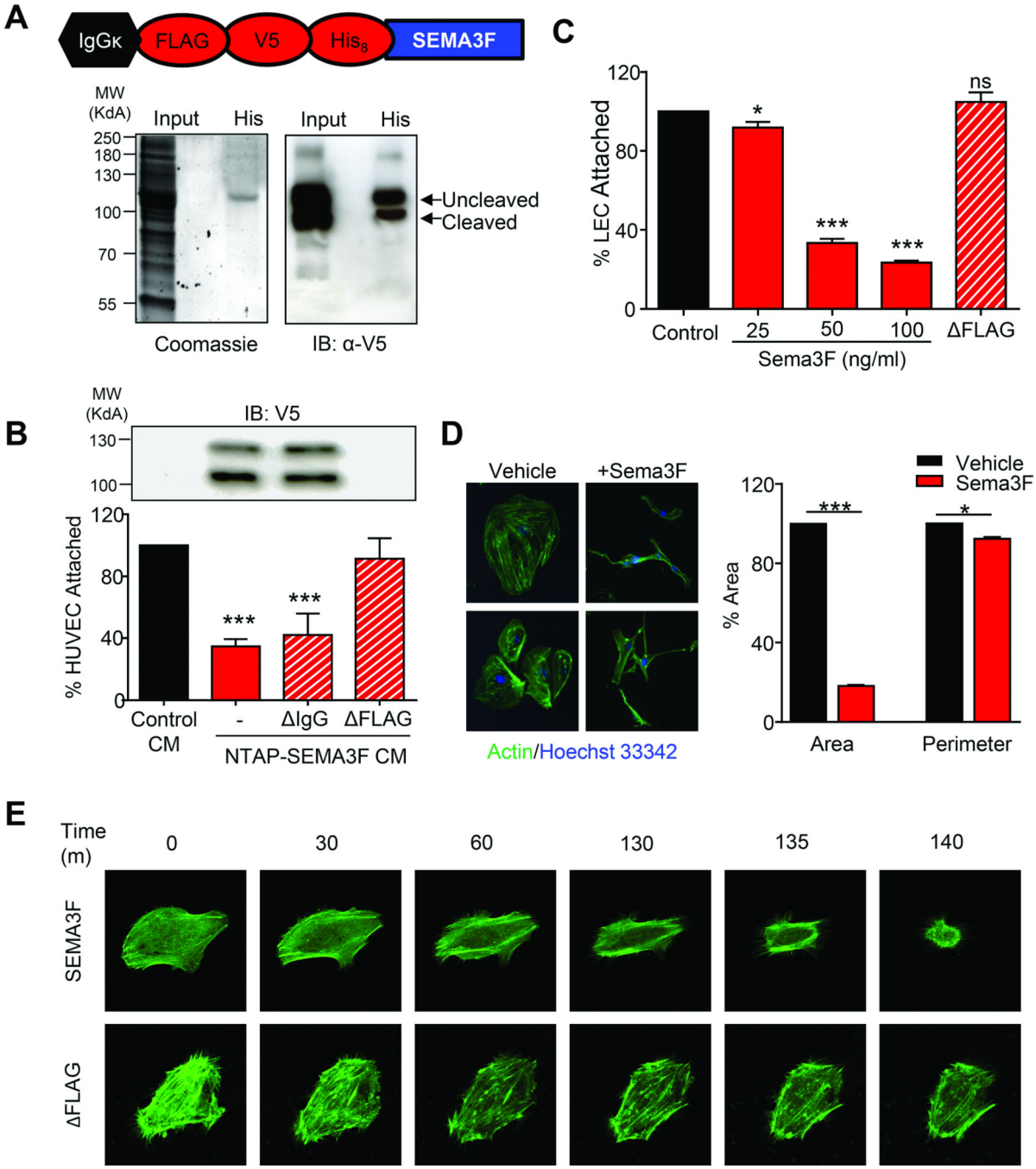

Fig. 2. SEMA3F is a chemorepulsant that negatively impacts the function of lymphatic endothelial cells

A) Coomassie staining and Western blot of serum-free CM from cells transfected with NTAP-SEMA3F. B) Attachment of HUVEC cells CM from NTAP-SEMA3F cell supernatants alone or after FLAG or IgG immunoprecipitation depletion. C) Attachment of LECs in the presence of increasing amounts of purified SEMA3F or supernatant after FLAG depletion. D) Immunofluorescent staining of actin (green) and nuclei (blue) in LEC treated with 100 ng/ml SEMA3F for 6 hours. Quantification of cell area and perimeter were determined using ImageJ using twenty-five independent fields. Statistical significance was

Author Manuscript Author Manuscript Author Manuscript Author Manuscript

determined using one-way ANOVA, *p<0.05, **p<0.01, ***p<0.001. E) Still images captured during live-cell imaging of LEC transfected with LifeAct GFP and treated with 1 μg/ml SEMA3F or ΔFLAG.

Author Manuscript Author Manuscript Author Manuscript Author Manuscript

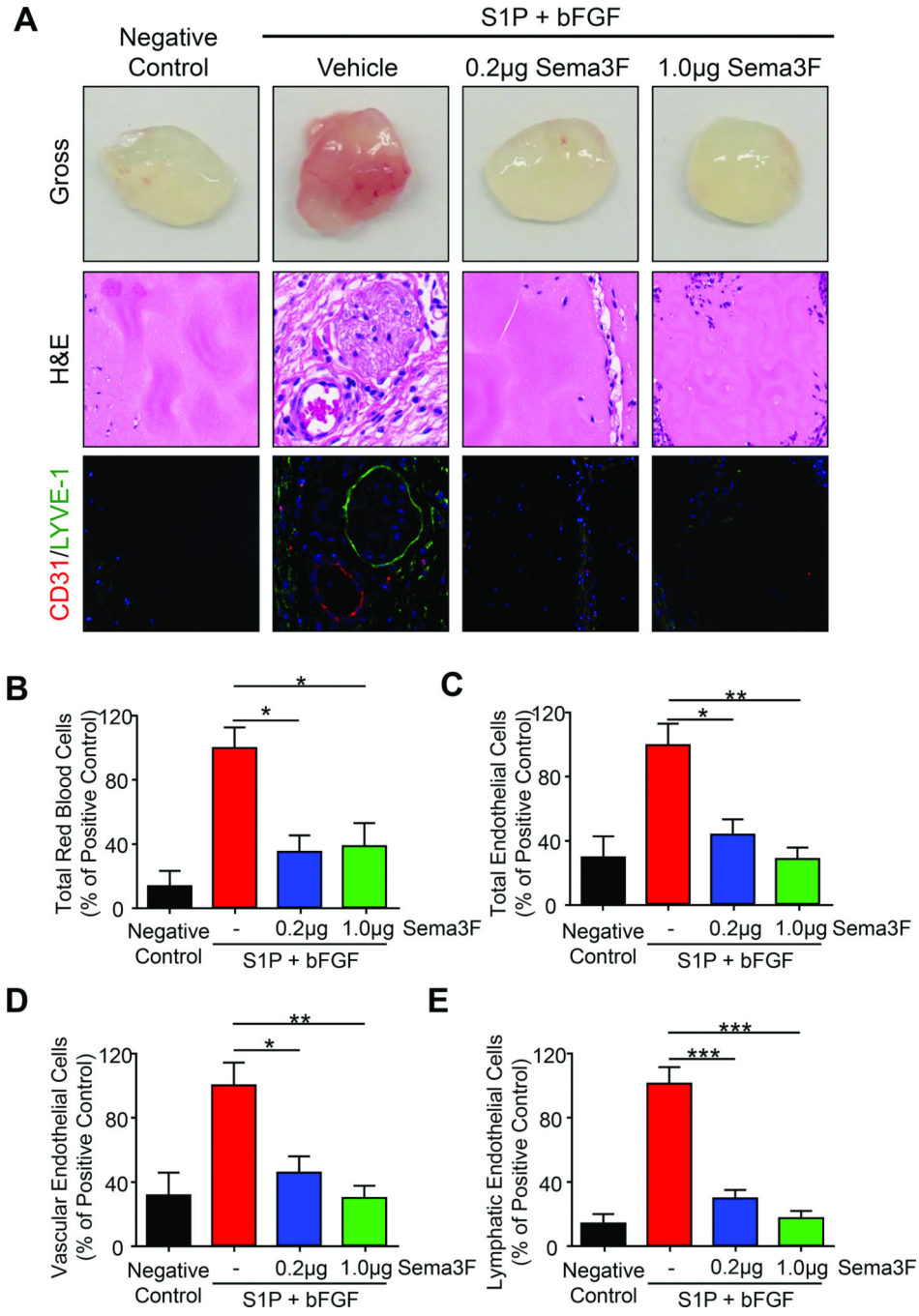

Fig. 3. SEMA3F inhibits *in vivo* lymphangiogenesis

A) Matrigel plugs containing the indicated factors were examined for gross histology (top row), H&E (middle row), and immunofluorescence for CD31 (red) and LYVE1 (green) (bottom row). FACS analysis of the number of total red blood cells (B), total $CD102^{+}CD31^{+}$ endothelial cells (C), LYVE-1^{low} vascular endothelial cells (D), and LYVE-1^{hi} lymphatic endothelial cells (E) are shown. Values were expressed as a percentage of the stimulated vehicle control from three independent experiments. Statistical significance was determined using one-way ANOVA, *$p<0.05$, **$p<0.01$, ***$p<0.001$.

Author Manuscript Author Manuscript Author Manuscript Author Manuscript

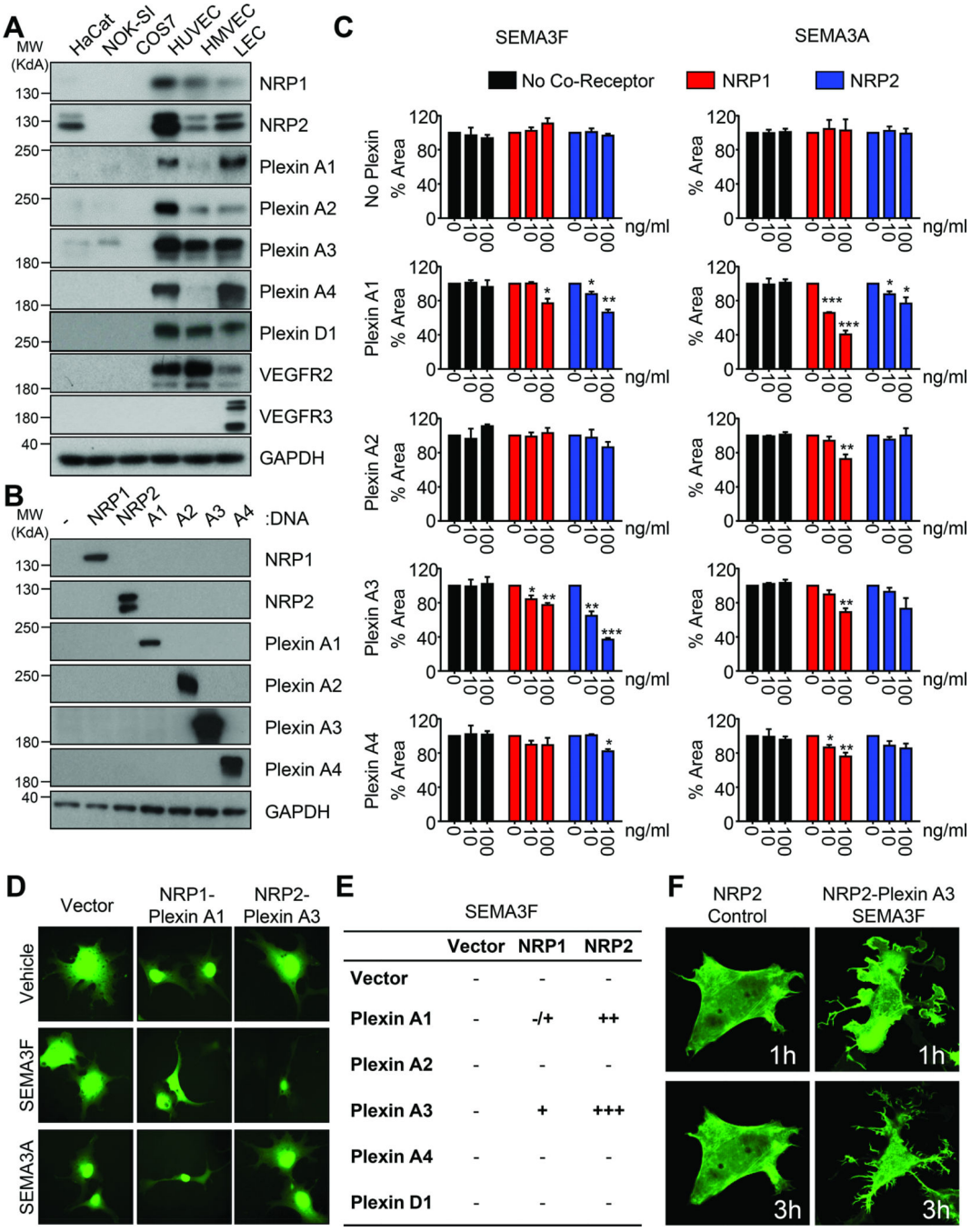

Fig. 4. NRP and Plexin A co-receptors coordinate SEMA3F function

A) Western blot demonstrating expression of the NRP, Plexin, and VEGFR family members in a panel of immortalized and primary epithelial and endothelial cells. B) Western blot demonstrated specific expression of each NRP and Plexin A family member in COS-7 cells. C) COS-7 cells stably expressing GFP were transfected and treated as indicated. Collapse was quantified using ImageJ relative to vehicle control based on 25 imaging fields each from quadruplicate wells in three independent experiments. Statistical significance was determined using one-way ANOVA, *p<0.05, **p<0.01, ***p<0.001. D) Representative

Author Manuscript Author Manuscript Author Manuscript Author Manuscript

images of cells transfected with different receptor combinations and treated with vehicle, SEMA3F, or SEMA3A. E) Table summarizing the relative contributions of the different receptor combinations tested. F) Confocal images of COS-7 cells transfected with LifeAct-GFP, NRP2, and/or Plexin A3 and treated with SEMA3F or ΔFLAG. Images were taken one hour and three hours after treatment with SEMA3F.

Author Manuscript Author Manuscript Author Manuscript Author Manuscript

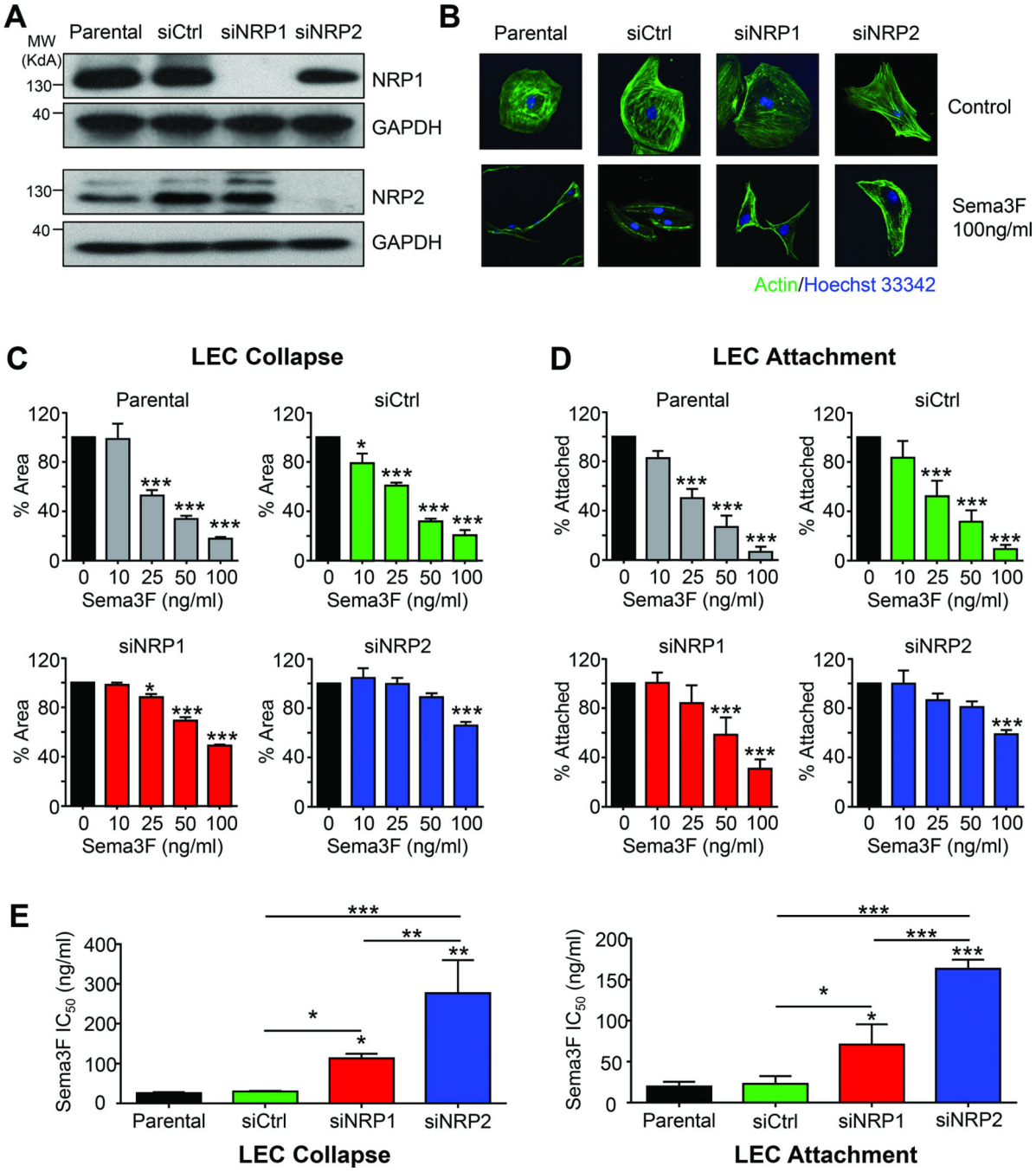

Fig. 5. NRP2 is predominantly required for SEMA3F function in LEC

A) Western blot of endogenous NRP1 and NRP2 in LEC in the presence of control (siCtrl), NRP1, or NRP2 siRNA. B) Fluorescent imaging of LEC transfected with the indicated siRNA and then treated with vehicle or 100 ng/ml SEMA3F. Parental and siCtrl-transfected LEC treated with increasing doses of SEMA3F and evaluated for collapse (C), or attachment (D) For both collapse and attachment assays, values are reported relative to vehicle control and quantification was done by ImageJ, based on 25 imaging fields each from quadruplicate wells in three independent experiments. E) IC_{50} of SEMA3F was calculated from the dose

curve generated in (C) and (D). Statistical significance was determined using one-way ANOVA, *p<0.05, **p<0.01, ***p<0.001.

Author Manuscript Author Manuscript Author Manuscript Author Manuscript

Author Manuscript Author Manuscript Author Manuscript Author Manuscript

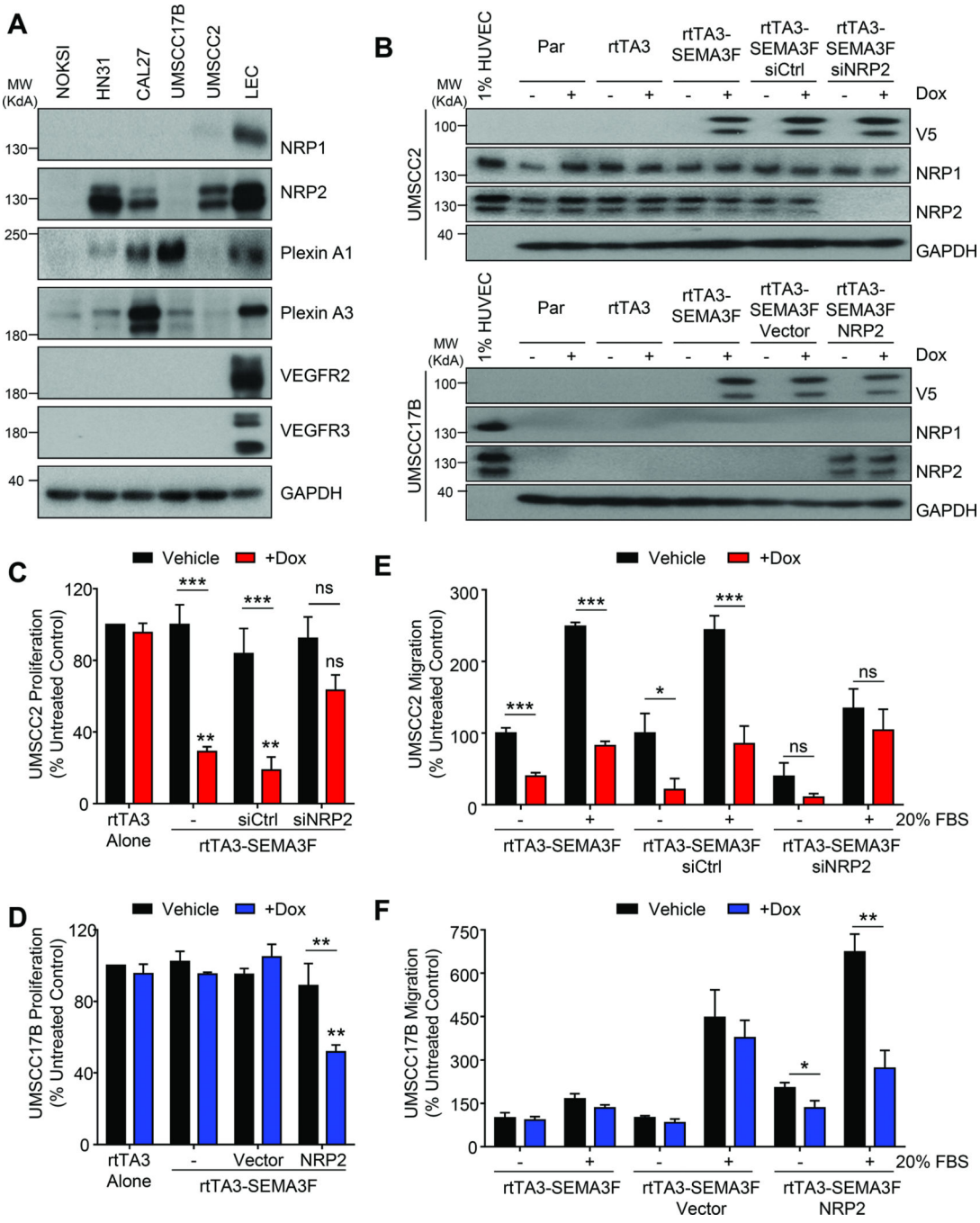

Fig. 6. NRP2 expression varies in HNSCC and mediates tumor cell responsiveness to SEMA3F

A) Western blot for the expression of receptors in normal oral keratinocytes (NOKSI) and panel of HNSCC cell lines. B) Western blot showing expression of inducible SEMA3F and knockdown or reintroduction of NRP2 expression in UMSCC2 and UMSCC17B cells, respectively. Proliferation assay of UMSCC2-rtTA3-SEMA3F (C) or UMSCC17B-rtTA3-SEMA3F (D) after SEMA3F induction. Cells were treated with control siRNA or NRP2 siRNA (C) or empty vector or NRP2 (D). Migration assay of UMSCC2-rtTA3-SEMA3F (E) or UMSCC17B-rtTA3-SEMA3F (F) cells with no stimulation (Vehicle) or towards 20%

FBS. Cells were treated with control siRNA or NRP2 siRNA (E) or empty vector or NRP2 (F). Proliferation and migration were reported as a percentage of control. Statistical significance was determined using one-way ANOVA, *p<0.05, **p<0.01, ***p<0.001.

Author Manuscript Author Manuscript Author Manuscript Author Manuscript

Author Manuscript Author Manuscript Author Manuscript Author Manuscript

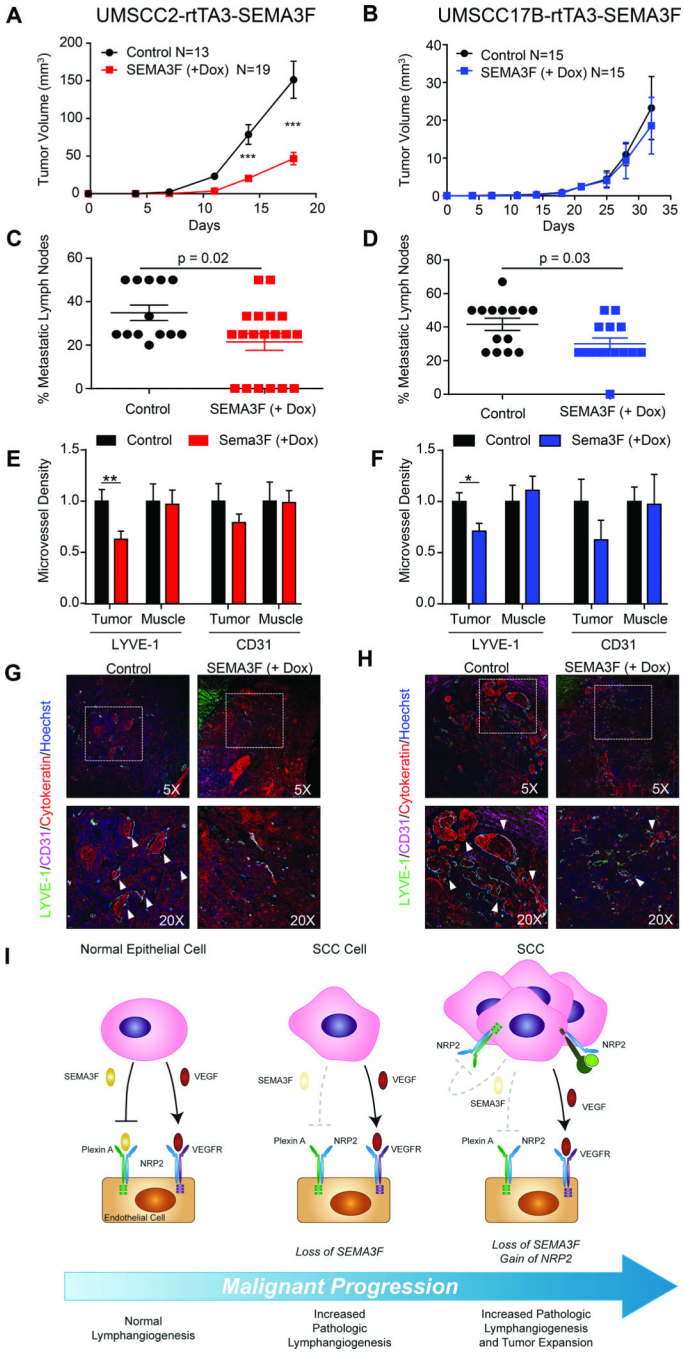

Fig. 7. SEMA3F functions as a tumor and metastasis suppressor *in vivo*

Tumor growth of UMSCC2-rtTA3-SEMA3F (A) and UMSCC17B-rtTA3-SEMA3F (B) after SEMA3F induction via doxy chow. Cervical lymph node metastasis was evaluated as the percentage of metastatic lymph nodes in control and doxy-fed animals for UMSCC2-rtTA3-SEMA3F (C) and UMSCC17B-rtTA3-SEMA3F (D). Microvessel density for lymphatic (LYVE-1) and blood (CD31) vessels was evaluated in the tumor and muscle of tongues for UMSCC2-rtTA3-SEMA3F (E) and UMSCC17B-rtTA3-SEMA3F (F). Microvessel density was reported relative to the average density in vessels/μm. Statistical

Author Manuscript Author Manuscript Author Manuscript Author Manuscript

significance was determined using Student's t-test, *p<0.05, **p<0.01, ***p<0.001. Immunofluorescent staining of tumors from control and doxy-fed animals for UMSCC2-rtTA3-SEMA3F (G) and UMSCC17B-rtTA3-SEMA3F (H) revealed a higher density and size of vessels in control animals. Lymphovascular invasion by cancer cells is indicated by white arrowheads. I) Proposed mechanism for the role of SEMA3F loss in HNSCC. See text for details.